

**JAERI-Research**  
**96-042**



**EVALUATION OF INDUCTIVE HEATING ENERGY OF SUB-SIZE  
IMPROVED DPC-U CONDUCTOR BY CALORIMETRIC METHOD**

**August 1996**

**Toshinobu ITO, Norikiyo KOIZUMI, Hiroshi WAKABAYASHI, Yuushi MIURA,  
Hiroshi FUJISAKI, Kunihiro MATSUI, Yoshikazu TAKAHASHI and Hiroshi TSUJI**

**日本原子力研究所**  
**Japan Atomic Energy Research Institute**

本レポートは、日本原子力研究所が不定期に公刊している研究報告書です。  
入手の間合わせは、日本原子力研究所研究情報部研究情報課（〒319-11 茨城県那珂郡東海村）あて、お申し越してください。なお、このほかに財団法人原子力弘済会資料センター（〒319-11 茨城県那珂郡東海村日本原子力研究所内）で複写による実費頒布をおこなっております。

This report is issued irregularly.

Inquiries about availability of the reports should be addressed to Research Information Division, Department of Intellectual Resources, Japan Atomic Energy Research Institute, Tokai-mura, Naka-gun, Ibaraki-ken, 319-11, Japan.

© Japan Atomic Energy Research Institute, 1996

編集兼発行 日本原子力研究所  
印 刷 いばらき印刷(株)

Evaluation of Inductive Heating Energy of Sub-size Improved DPC-C  
Conductor by Calorimetric Method

Toshinobu ITO, Norikiyo KOIZUMI, Hiroshi WAKABAYASHI, Yuushi MIURA,  
Hiroshi FUJISAKI, Kunihiro MATSUI, Yoshikazu TAKAHASHI and Hiroshi TSUJI

Department of Fusion Engineering Research  
Naka Fusion Research Establishment  
Japan Atomic Energy Research Institute  
Naka-machi, Naka-gun, Ibaraki-ken

(Received July 5, 1996)

The improved DPC-U conductor consisting of 648 chrome plated NbTi strands was fabricated and its stability has been investigated using 1/24 sub-size conductor. In the stability experiment, the inductive heating method was applied to originate initial normal zone. Since it is difficult to calculate the inductive heating energy deposited on the conductor because of complicate geometry of the twisted multi-strand cable, inductive heating energy had to be experimentally evaluated using calorimetric method. The heating energy is in proportion to integration of square of an applied sinusoidal wave pulsed current over the heating period. The experimental result shows the proportional constants for the conductor and conduit are  $2.062 \times 10^{-3}$  [J/A<sup>2</sup>s] and  $0.771 \times 10^{-3}$  [J/A<sup>2</sup>s], respectively. The coupling between the eddy currents in the strands and conduit might take effect on the heating energy put in the strands. It was shown this effect was however small in this experiment. Consequently, the inductive heating energy applied in the strands was estimated to be the proportional constant of  $1.291 \times 10^{-3}$  [J/A<sup>2</sup>s] from the difference of the heat energies in the conductor and conduit.

Keywords: Superconductor, Stability, Inductive Heating, Calorimetric

熱量法による改良DPC-U縮小導体の誘導加熱量の評価

日本原子力研究所那珂研究所核融合工学部

伊藤 智庸・小泉 徳潔・若林 宏・三浦 友史  
藤崎 礼志・松井 邦浩・高橋 良和・辻 博史

(1996年7月5日受理)

648本のNbTi・クロムメッキ素線を用いた改良DPC-U導体を製作し、その安定性を1/24縮小導体を用いて評価した。安定性実験では、誘導加熱法により初期の擾乱を印加した。導体に投入された誘導加熱量は、導体を構成する撚線ケーブルの形状が複雑なため、計算で求めることができない。そこで、熱量法により誘導加熱量の評価を行った。誘導ヒータには正弦波電流を流したため、誘導加熱エネルギーは、ヒータ電流の平方の時間積分に比例した。導体およびコンジットの誘導加熱に対して、その比例定数は、それぞれ  $2.062 \times 10^{-3} [\text{J}/\text{A}^2\text{s}]$  および  $0.771 \times 10^{-3} [\text{J}/\text{A}^2\text{s}]$  となった。誘導加熱では、素線内の渦電流とコンジット内の渦電流の結合が、素線の誘導加熱量に影響を及ぼすことがある。しかし、本実験では、渦電流の結合による影響は小さいことが示された。したがって、導体の誘導加熱量からコンジットの誘導加熱量を引くことによって、素線の誘導加熱量が求まる。素線の誘導加熱量の比例定数は、 $1.291 \times 10^{-3} [\text{J}/\text{A}^2\text{s}]$  と評価できた。

## Contents

1. Introduction .....	1
2. Major Parameters of the Sample Conductor .....	2
3. Experimental Method .....	2
4. Experimental Results .....	6
5. Data Analysis .....	8
5.1 Effect of the Coupling between Eddy Currents in the Cable and Conduit .....	8
5.2 Correction of Heat Energy .....	12
6. Conclusion .....	13
Acknowledgments .....	13
References .....	13

## 目 次

1. はじめに .....	1
2. サンプル導体主要緒言 .....	2
3. 実験方法 .....	2
4. 実験結果 .....	6
5. データ解析 .....	8
5.1 素線およびコンジット内渦電流の結合の影響 .....	8
5.2 加熱量の較正 .....	12
6. 結 論 .....	13
謝 辞 .....	13
参考文献 .....	13

## 1. Introduction

The Demo Poloidal Coil (DPC) Project<sup>1</sup> which was started in 1985 at Japan Atomic Energy Research Institute (JAERI) was set up for purpose of developing and studying large, forced-flow cooling and Cable-in-Conduit (CIC) superconducting poloidal coils for next generation fusion reactors. In this project, two 30 kA NbTi coils, DPC-U1 and U2<sup>2-4</sup>, were fabricated to demonstrate the applicability of superconducting technology to a pulsed coil and provide a background field for Nb<sub>3</sub>Sn tested coils<sup>5-7</sup> to be installed between DPC-U1 and -U2. ( Hereafter DPC-U1 and -U2 will collectively be called DPC-U.) However, DPC-U exhibited instability such as the conductor quenches at 40% of the design current. It was found that this instability was caused by a current imbalance which was generated in the DPC-U conductor during the charging of the coil since the current could not be transferred among the strands coated by formvar when the normalcy appears<sup>2-4</sup>.

The improved DPC-U conductor<sup>8</sup> consisting of 648 chrome plated NbTi strands was fabricated to remove this instability and its stability were investigated using a 1/24 sub-size conductor<sup>9,10</sup>. In the stability experiment, the conductor was heated using an inductive heater to produce an initial normal zone.

The inductive heating method seems the most suitable for simulating an actual perturbation in a stability experiment since the conductor can directly be heated without any time delay. However, the heat energy deposited in the conductor by inductive heating cannot be evaluated by calculation because of complicated geometry of the conductor. Therefore, the heat energy generated by inductive heating was evaluated experimentally.

The calorimetric method, which is usually used for AC loss measurements<sup>11</sup>, was employed for evaluation of inductive heating energy. This technique has been successfully demonstrated in the zero magnetic field<sup>2</sup>. However, the inductive heating energy is affected by an applied magnetic field. Therefore, the evaluation of the inductive heating energy should be carried out in the same magnetic field, 7 T, at which the stability experiment was performed<sup>9,10</sup>.

It is significant for studying the stability to evaluate how heat energy is deposited on the strands and conduit<sup>9</sup>. Therefore, an attempt was made to estimate the heat energy

deposited on the strands and conduit.

This report describes the evaluation results of inductive heating energy.

## 2. Major Parameters of the Sample Conductor

The sample conductor is a CIC conductor having 27 NbTi strands developed for a pulse coil. The strands have NbTi/CuNi/Cu three layered structure to reduce the coupling losses among the NbTi filaments. In addition, the strands are plated with chromium to reduce coupling losses among the strands. The conduit is made of stainless steel. The length of the sample conductor is 9 cm. *Table 1* shows the major parameters of the sample conductor. *Figures 1* and *2* show a cross-sectional view of the sample conductor and strand, respectively.

## 3. Experimental Method

A sinusoidal wave magnetic field pulse was applied to the conductor in the stability experiment<sup>9,10</sup>. Then, the current to the inductive heater,  $I_h$  [A], is represented by,

$$I_h = I_{hp} \sin(2\pi ft). \quad (1)$$

Where  $I_{hp}$  [A] and  $f$  [Hz] denote the amplitude and frequency of the inductive heater's current pulse, respectively. The effective heating power by inductive heating with a sinusoidal wave pulse is in proportion to the square of the amplitude of the magnetic field<sup>12</sup>. The inductive heating energy,  $E_h$  [J], is consequently evaluated by,

Table 1. The major parameters of the sample conductor

Superconductor material	NbTi
NbTi filament diameter	10 $\mu$ m
NbTi / Cu / CuNi	1 / 3.88 / 1.07
Strands diameter	1.115 mm
Strand surface	5 $\mu$ m chrome plating
Residual resistance ratio	53
Number of strands	27
Void faction	36.8%
Inner diameter of the conduit	7.41 mm
Outer diameter of the conduit	9.61 mm
Conduit material	Stainless steel
Conductor length	90 mm

deposited on the strands and conduit.

This report describes the evaluation results of inductive heating energy.

## 2. Major Parameters of the Sample Conductor

The sample conductor is a CIC conductor having 27 NbTi strands developed for a pulse coil. The strands have NbTi/CuNi/Cu three layered structure to reduce the coupling losses among the NbTi filaments. In addition, the strands are plated with chromium to reduce coupling losses among the strands. The conduit is made of stainless steel. The length of the sample conductor is 9 cm. *Table 1* shows the major parameters of the sample conductor. *Figures 1* and *2* show a cross-sectional view of the sample conductor and strand, respectively.

## 3. Experimental Method

A sinusoidal wave magnetic field pulse was applied to the conductor in the stability experiment<sup>9,10</sup>. Then, the current to the inductive heater,  $I_h$  [A], is represented by,

$$I_h = I_{hp} \sin(2\pi ft). \quad (1)$$

Where  $I_{hp}$  [A] and  $f$  [Hz] denote the amplitude and frequency of the inductive heater's current pulse, respectively. The effective heating power by inductive heating with a sinusoidal wave pulse is in proportion to the square of the amplitude of the magnetic field<sup>12</sup>. The inductive heating energy,  $E_h$  [J], is consequently evaluated by,

Table 1. The major parameters of the sample conductor

Superconductor material	NbTi
NbTi filament diameter	10 $\mu$ m
NbTi / Cu / CuNi	1 / 3.88 / 1.07
Strands diameter	1.115 mm
Strand surface	5 $\mu$ m chrome plating
Residual resistance ratio	53
Number of strands	27
Void faction	36.8%
Inner diameter of the conduit	7.41 mm
Outer diameter of the conduit	9.61 mm
Conduit material	Stainless steel
Conductor length	90 mm

deposited on the strands and conduit.

This report describes the evaluation results of inductive heating energy.

## 2. Major Parameters of the Sample Conductor

The sample conductor is a CIC conductor having 27 NbTi strands developed for a pulse coil. The strands have NbTi/CuNi/Cu three layered structure to reduce the coupling losses among the NbTi filaments. In addition, the strands are plated with chromium to reduce coupling losses among the strands. The conduit is made of stainless steel. The length of the sample conductor is 9 cm. *Table 1* shows the major parameters of the sample conductor. *Figures 1* and *2* show a cross-sectional view of the sample conductor and strand, respectively.

## 3. Experimental Method

A sinusoidal wave magnetic field pulse was applied to the conductor in the stability experiment<sup>9,10</sup>. Then, the current to the inductive heater,  $I_h$  [A], is represented by,

$$I_h = I_{hp} \sin(2\pi ft). \quad (1)$$

Where  $I_{hp}$  [A] and  $f$  [Hz] denote the amplitude and frequency of the inductive heater's current pulse, respectively. The effective heating power by inductive heating with a sinusoidal wave pulse is in proportion to the square of the amplitude of the magnetic field<sup>12</sup>. The inductive heating energy,  $E_h$  [J], is consequently evaluated by,

Table 1. The major parameters of the sample conductor

Superconductor material	NbTi
NbTi filament diameter	10 $\mu$ m
NbTi / Cu / CuNi	1 / 3.88 / 1.07
Strands diameter	1.115 mm
Strand surface	5 $\mu$ m chrome plating
Residual resistance ratio	53
Number of strands	27
Void faction	36.8%
Inner diameter of the conduit	7.41 mm
Outer diameter of the conduit	9.61 mm
Conduit material	Stainless steel
Conductor length	90 mm

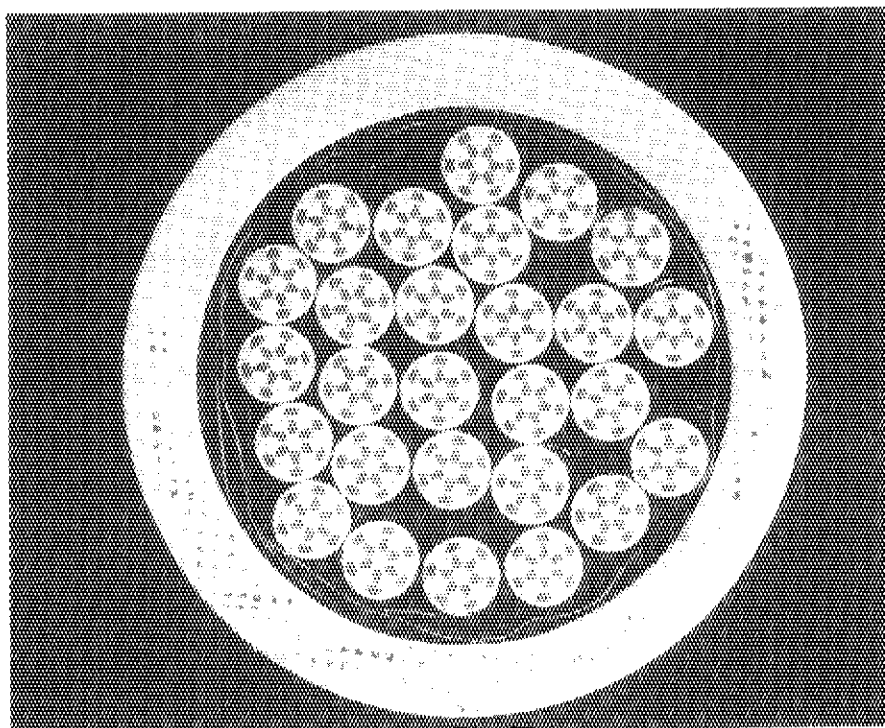


Fig. 1. Cross-sectional view of the sample conductor.

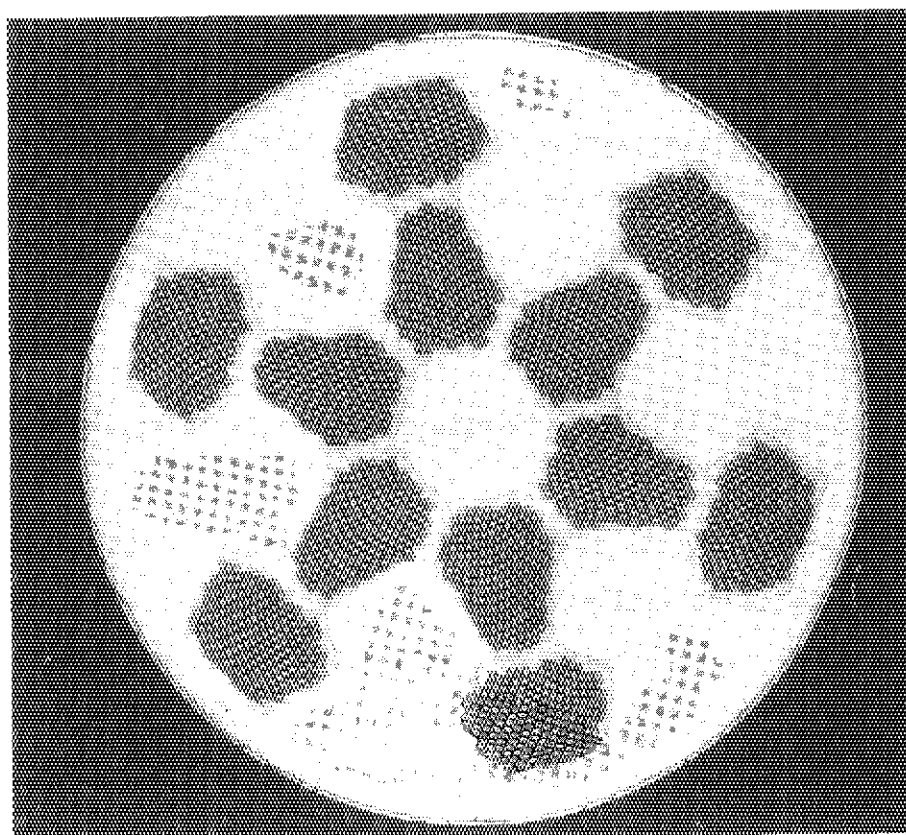


Fig. 2. Cross-sectional view of the strand.

$$E_h = C \int_0^{t_h} I_h^2 dt = \frac{CI_{hp}^2 t_h}{2}. \quad (2)$$

Where  $t_h$  [s] denotes the heating period. Hereinafter  $\int_0^{t_h} I_h^2 dt$  [A<sup>2</sup>s] is referred to as the heating factor, for simplicity sake. The purpose of this experiment is to evaluate the proportional constant,  $C$  [J/A<sup>2</sup>s], in Eq. (2).

When the heat energy is deposited on the conductor immersed in the liquid helium (LHe), LHe is vaporized around the conductor. The volume of the vaporized gas helium (GHe) is proportional to the input heat energy. Proportional constant  $C$  is evaluated by observing the volume of the vaporized GHe.

The vaporized GHe is collected into the chamber located above the conductor as shown in *Fig. 3*. Since the volume of the vaporized GHe is proportional to the decrease of the LHe surface level in the chamber, the heat energy that has been deposited on the conductor can be evaluated by measuring the reduction of the LHe level in the chamber. The reduction in the LHe level in the chamber is measured by the LHe level meter installed in the chamber as shown in *Fig. 3*.

The relation between the reduction of the LHe level in the chamber and the input heat energy is calibrated using the resistive heater installed beside the GFP holder in which the sample conductor places as can be seen in *Fig. 3*. The heat energy by the resistive heater,  $E_{hr}$  [J], is calculated from,

$$E_{hr} = \int_0^{t_h} I_{hr} \cdot V_{hr} dt. \quad (3)$$

Where  $I_{hr}$  [A] and  $V_{hr}$  [V] denote the measured current and voltage of the resistive heater.

The heating period, frequency and magnetic field were from 5 to 40 ms, 1 kHz and 7 T, respectively, during the stability experiment. In this experiment, the frequency was set at 1 kHz, but the heating duration was fixed at 30 ms since inductive heating energy for other heating duration can be estimated from Eq. (2) if the heating energy is measured for a certain heating period. The magnetic field of 7 T is subjected to the sample conductor from a backup coil which can provide a magnetic field up to 13 T on the conductor.

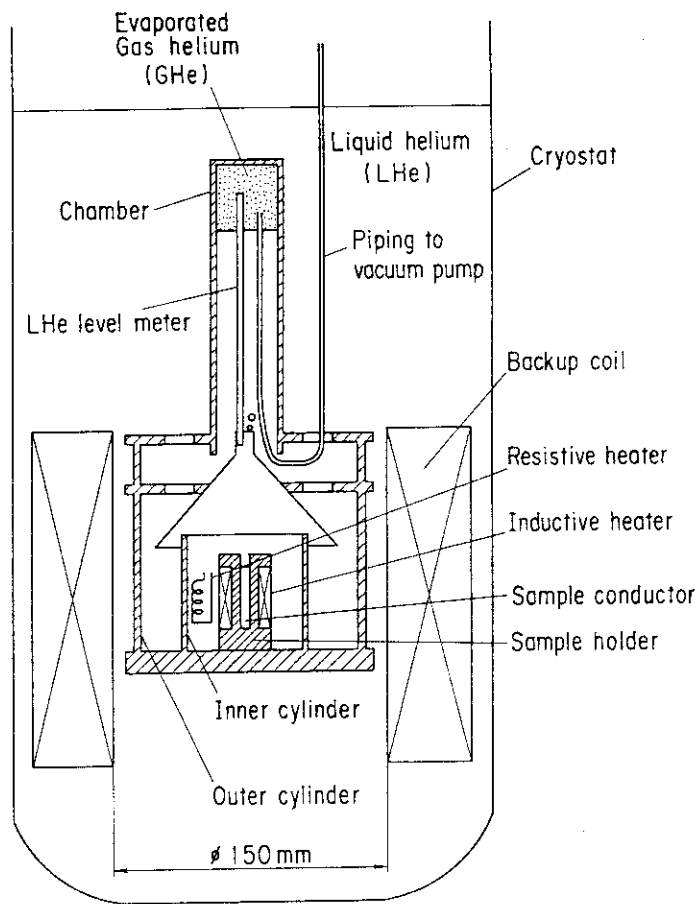


Fig. 3. Schematic configuration of the experimental device. GHe evaporated by inductive or resistive heating is prevented from leaving the chamber due to the inner cylinder. The outer cylinder avoids the generation of GHe except for inductive and resistive heating coming into the chamber. GHe that has collected in the chamber can be absorbed by a vacuum pump through the piping install in the chamber.

In the experiment, the Joule heating energy of the inductive heater vaporized LHe. The Joule heating energy of the inductive heater should be measured to separate it from the inductive heating energy put in the conductor.

Since the strand is designed for a pulse coil<sup>8</sup>, the heat energy generated in the cable by inductive heating is not large. The eddy current loss in the conduit is not negligible in comparison with that in the cable. The heat energy put in the conduit has an influence on the stability of the conductor. The inductive heating energy in the conduit should therefore be evaluated to precisely study the stability of this conductor<sup>9</sup>.

Consequently, it is required to evaluate the heat energies generated by putting the inductive heating pulse for the following samples.

- 1) The conductor and inductive heater;

- 2) the conduit and inductive heater; and
- 3) the inductive heater alone.

The LHe level in the chamber decreases after heat input but thereafter increases slightly. This is probably because of GHe liquidizing in the chamber. The increment rate of the LHe level strongly depended on the pressure in the chamber. It took more than several hours between each measurement of the above case for substitution of the sample. The pressure in the chamber might change between the measurements as a result of a variation in atmosphere pressure. Therefore, we were afraid the rate of the LHe level increase in the chamber was different among these measurements. The calibration of the heat energy by the resistive heater was carried out for each sample to eliminate any such calibration errors.

It takes certain duration to completely exchange the heat energy deposited in the conductor or the resistive heater to evaporation energy from LHe to GHe. The reduction of the LHe level was consequently measured after long elapse of time, 72 s, from the onset of the inductive or resistive heatings.

#### 4. Experimental Results

*Figure 4* shows the calibration results of the relations between the reduction in the LHe level and the heat energy by the resistive heater. The LHe level reduction for zero heating energy corresponds to the increase in the LHe level due to liquidizing and they are slightly different among three samples. However, the relations between them show very good linearity and almost coincide. The good linearity shows that the input heat energy is proportional to the LHe level reduction. In addition, good agreement of those relations shows there was no serious variation in the pressure in the chamber, resulting in no scatter due to a pressure variation in the calibrated relations, during the experiment.

Using these calibration results and the measured relation between the LHe level reduction and the heating factor, the relations between the inductive heating energy and the heating factor could be obtained.

*Figure 5* shows the evaluated results. The inductive heating energy proportionally increases as a function of the heating factor for all cases. This supports the validity of

- 2) the conduit and inductive heater; and
- 3) the inductive heater alone.

The LHe level in the chamber decreases after heat input but thereafter increases slightly. This is probably because of GHe liquidizing in the chamber. The increment rate of the LHe level strongly depended on the pressure in the chamber. It took more than several hours between each measurement of the above case for substitution of the sample. The pressure in the chamber might change between the measurements as a result of a variation in atmosphere pressure. Therefore, we were afraid the rate of the LHe level increase in the chamber was different among these measurements. The calibration of the heat energy by the resistive heater was carried out for each sample to eliminate any such calibration errors.

It takes certain duration to completely exchange the heat energy deposited in the conductor or the resistive heater to evaporation energy from LHe to GHe. The reduction of the LHe level was consequently measured after long elapse of time, 72 s, from the onset of the inductive or resistive heatings.

#### 4. Experimental Results

*Figure 4* shows the calibration results of the relations between the reduction in the LHe level and the heat energy by the resistive heater. The LHe level reduction for zero heating energy corresponds to the increase in the LHe level due to liquidizing and they are slightly different among three samples. However, the relations between them show very good linearity and almost coincide. The good linearity shows that the input heat energy is proportional to the LHe level reduction. In addition, good agreement of those relations shows there was no serious variation in the pressure in the chamber, resulting in no scatter due to a pressure variation in the calibrated relations, during the experiment.

Using these calibration results and the measured relation between the LHe level reduction and the heating factor, the relations between the inductive heating energy and the heating factor could be obtained.

*Figure 5* shows the evaluated results. The inductive heating energy proportionally increases as a function of the heating factor for all cases. This supports the validity of

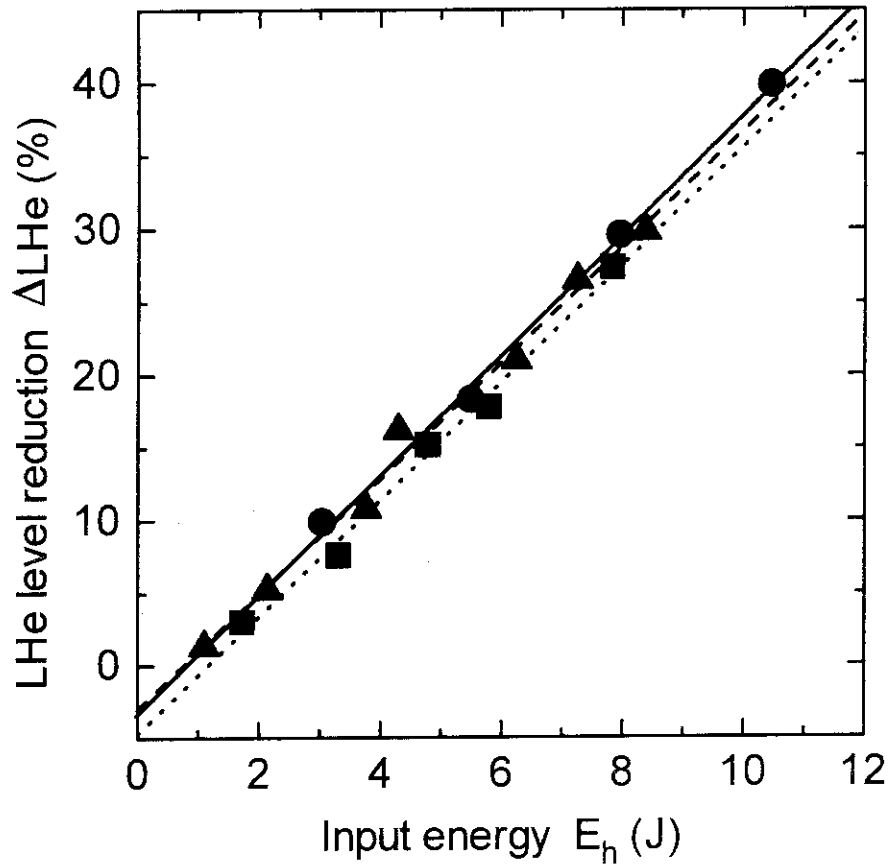


Fig. 4. Relation between the heat energy by the resistive heater and reduction in the LHe level. Circles, triangles and squares show the heat energy for the samples of the conductor and inductive heater, the conduit and inductive heater and the inductive heater alone, respectively. Solid, dash and dot lines show an approximation by least squares method.

Eq. (2). From these results, the following equations were obtained.

1) For the conductor and inductive heater,

$$E_h = 5.404 \times 10^{-3} \int_0^h I_h^2 dt. \quad (4)$$

2) For the conduit and inductive heater,

$$E_h = 4.113 \times 10^{-3} \int_0^h I_h^2 dt. \quad (5)$$

3) For the inductive heater alone,

$$E_h = 3.342 \times 10^{-3} \int_0^h I_h^2 dt. \quad (6)$$

The heat energy deposited in the conductor and conduit are estimated by subtracting Eq. (6) from Eqs. (4) and (5) in the following way.

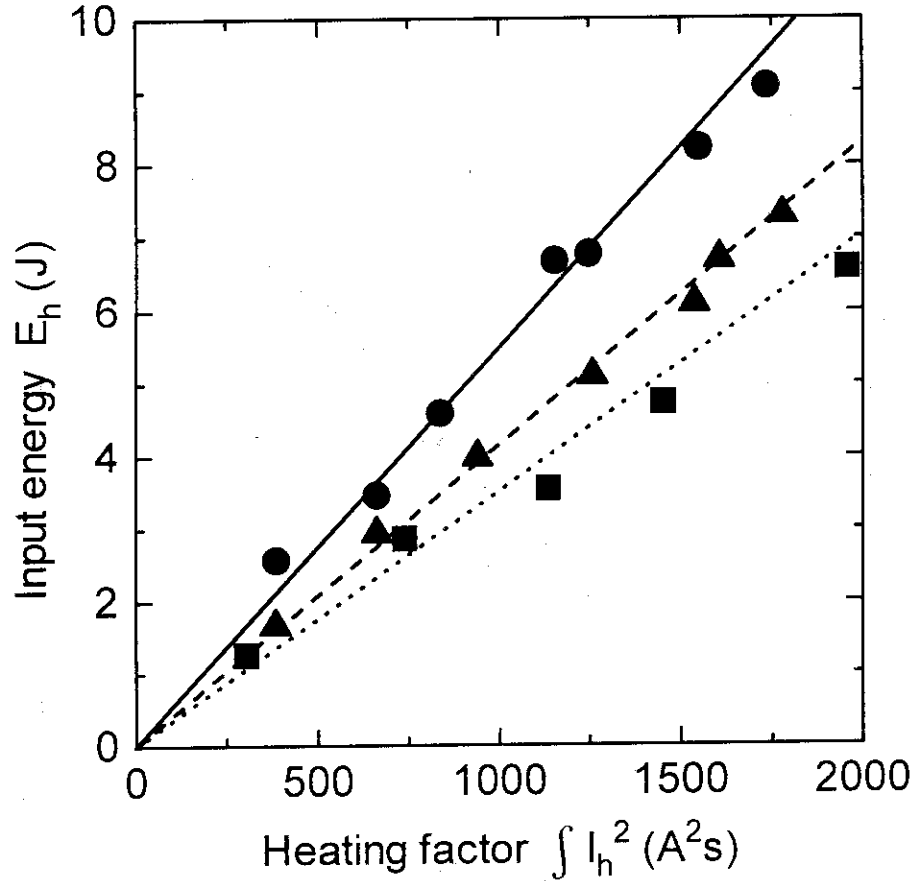


Fig. 5. The inductive heating energy as a function of the heating factor. Circles, triangles and squares show the heat energy for the samples of the conductor and inductive heater, the conduit and inductive heater and the inductive heater alone, respectively. Solid, dash and dot lines show the inductive heating energy calculated by Eqs. (5), (6) and (7), respectively.

a) For the conductor,

$$E_h = 2.062 \times 10^{-3} \int_0^h I_h^2 dt. \quad (7)$$

b) For the conduit,

$$E_h = 0.771 \times 10^{-3} \int_0^h I_h^2 dt. \quad (8)$$

## 5. Data Analysis

### 5.1 Effect of the coupling between the eddy currents in the strands and conduit

The eddy currents induced in the strands reduce the applied magnetic flux. The magnetic flux passing through the area enclosed by the conduit is therefore made smaller in case the strands exist in the conduit than the one with no strands<sup>12</sup>. This

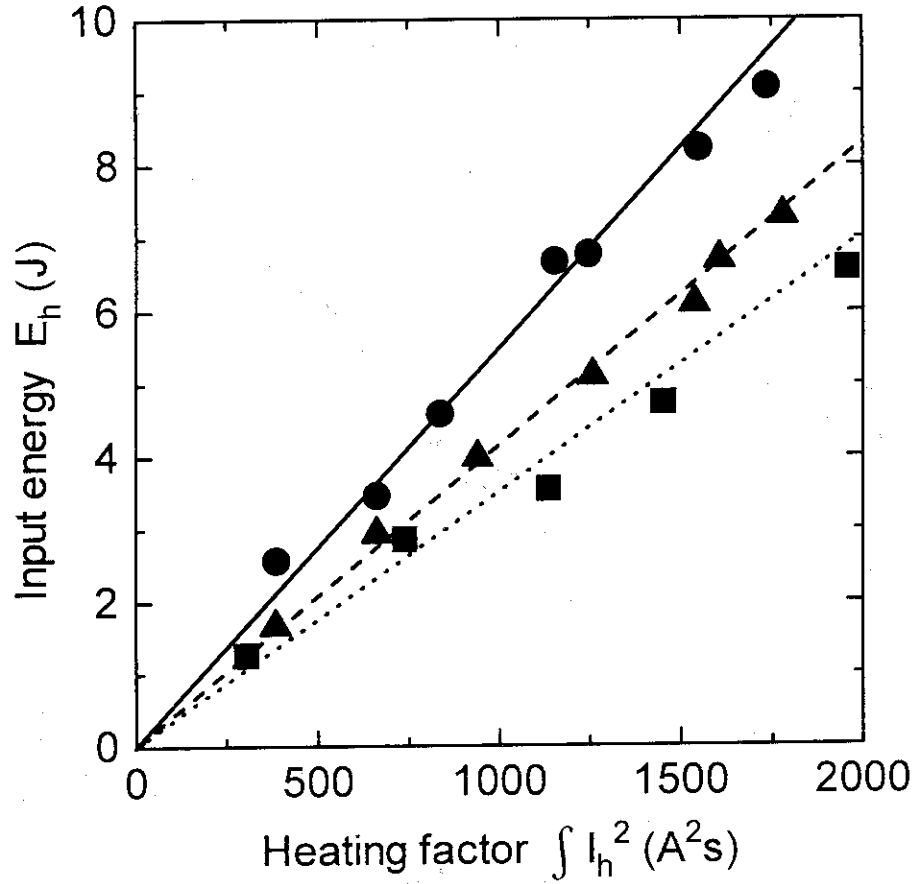


Fig. 5. The inductive heating energy as a function of the heating factor. Circles, triangles and squares show the heat energy for the samples of the conductor and inductive heater, the conduit and inductive heater and the inductive heater alone, respectively. Solid, dash and dot lines show the inductive heating energy calculated by Eqs. (5), (6) and (7), respectively.

a) For the conductor,

$$E_h = 2.062 \times 10^{-3} \int_0^h I_h^2 dt. \quad (7)$$

b) For the conduit,

$$E_h = 0.771 \times 10^{-3} \int_0^h I_h^2 dt. \quad (8)$$

## 5. Data Analysis

### 5.1 Effect of the coupling between the eddy currents in the strands and conduit

The eddy currents induced in the strands reduce the applied magnetic flux. The magnetic flux passing through the area enclosed by the conduit is therefore made smaller in case the strands exist in the conduit than the one with no strands<sup>12</sup>. This

indicates the eddy current loss becomes smaller in the former case than the latter. The inductive heating energy of the strands could not therefore be accurately estimated by subtracting the heat energy in the conduit from that in the conductor. The effect from coupling of the eddy currents in the strands and conduit is studied to show this effect is negligibly small in this experiment.

A three-dimensional simulation should be carried out for accurate estimation of the eddy currents in the strands and conduit. However, a three-dimensional simulation is difficult and seems impossible because of the complicated geometry of the cable. We employ a one-dimensional cylinder model for sake of simplicity. This simple model is sufficient to verify that the coupling of the eddy currents does not have an influence on the heating energy.

The conductance between the chrome plated strands has been measured to be  $10^3$  S/m by Ono *et al.*<sup>13</sup>. The conductance is so small that the small eddy currents are induced among the strands. The eddy currents in the strands therefore dominate the heat energy in the cable. Since the superconducting filaments are surrounded by a CuNi layer, the coupling current among the filaments is also small. On the other hand, there exists a relatively large loop, that is a copper layer near the strand surface, in the copper cross section as shown in Fig. 2. The most effective eddy current in the cable is thought to be induced in this copper layer. The thickness of this layer is about 50  $\mu\text{m}$  at its minimum.

It is assumed the eddy currents induced in the conduit and copper layer in the strands are uniform on each cross section and the conductor is placed in a uniform magnetic field whose direction is the same as the conductor axis. Also, the strands are supposed to be straight and their axis is in the same direction as the magnetic field. These assumptions make the analysis of the coupling of the eddy currents in the strands and conduit possible. The governing equations for the eddy currents become as follows:

$$\begin{aligned} S_{st} \frac{d(B_0 - B_{st} - B_{con})}{dt} &= R_{st} I_{st}, \\ S_{con} \frac{d(B_0 - NS_{st} B_{st} / S_{con} - B_{con})}{dt} &= R_{con} I_{con}. \end{aligned} \quad (9)$$

Where  $S$  [ $\text{m}^2$ ] denote cross-sectional area where the magnetic flux passes,  $B$  [T] the magnetic field,  $R$  [ $\Omega$ ] the resistance of the loop,  $I$  [A] the eddy current and  $N$  the

number of the strands, respectively. Subscripts *st* and *con* indicate the values are for the strands and conduit, respectively.  $B_0$  [T] is the magnetic field from the inductive heater. Note that the eddy currents in the strands are supposed to flow in a mere 50  $\mu\text{m}$  thick copper layer near the surface of the strands.

The magnetic fields from the eddy currents in the strands and conduit are calculated by,

$$\begin{aligned} B_{st} &= \mu_0 I_{st} / L, \\ B_{con} &= \mu_0 I_{con} / L. \end{aligned} \quad (10)$$

The applied magnetic field can be written in the following way.

$$B_0 = B_p e^{j\omega t}. \quad (11)$$

Where  $B_p$  [T] and  $\omega$  [Hz] denote the amplitude and radial frequency of the applied inductive heating pulse, respectively. Substituting Eqs. (10) and (11) into Eq. (9), one has,

$$\frac{dI_{st}}{dt} + \frac{dI_{con}}{dt} + \frac{R_{st}L}{\mu_0 S_{st}} I_{st} + \frac{j\omega B_p L}{\mu_0} e^{j\omega t} = 0, \quad (12)$$

$$\alpha \frac{dI_{st}}{dt} + \frac{dI_{con}}{dt} + \frac{R_{con}L}{\mu_0 S_{con}} I_{con} + \frac{j\omega B_p L}{\mu_0} e^{j\omega t} = 0.$$

$$\alpha = NS_{st}/S_{con}. \quad (13)$$

Equation (12) can be rewritten using the vector expression as follows.

$$\frac{d\mathbf{i}}{dt} + \mathbf{A}\mathbf{i} + \frac{j\omega B_p L}{\mu_0} e^{j\omega t} \mathbf{x} = \mathbf{0}. \quad (14)$$

Where,

$$\mathbf{A} = a \begin{pmatrix} \gamma_{st} & -\gamma_c \\ -\alpha\gamma_{st} & \gamma_c \end{pmatrix}, \quad \mathbf{i} = \begin{pmatrix} I_{st} \\ I_{con} \end{pmatrix}, \quad \mathbf{x} = \begin{pmatrix} 0 \\ 1 \end{pmatrix}. \quad (15)$$

$$\gamma_{st} = \frac{R_{st}}{S_{st}}, \quad \gamma_{con} = \frac{R_{con}}{S_{con}}, \quad a = \frac{L}{\mu_0(1-\alpha)} \quad (16)$$

The eddy currents in a steady state can be calculated by<sup>14</sup>,

$$\mathbf{i} = \frac{\omega B_p L}{\mu_0} e^{j\omega t} \left( \frac{-\omega + j\lambda_1}{\omega^2 + \lambda_1^2} \mathbf{P}_1 + \frac{-\omega + j\lambda_2}{\omega^2 + \lambda_2^2} \mathbf{P}_2 \right) \mathbf{x} \quad (17)$$

Where  $\lambda_1$  and  $\lambda_2$  denote the eigen values for matrix  $\mathbf{A}$ , and  $\mathbf{P}_1$  and  $\mathbf{P}_2$  are the eigen projection matrices<sup>15</sup>.

$$\lambda_1 = \frac{a[-(\gamma_{st} + \gamma_{con}) + \sqrt{D}]}{2}, \quad \lambda_2 = \frac{a[-(\gamma_{st} + \gamma_{con}) - \sqrt{D}]}{2} \quad (18)$$

$$\mathbf{P}_1 = \frac{1}{2\sqrt{D}} \begin{pmatrix} -C + \sqrt{D} & 2\gamma_{con} \\ 2\alpha\gamma_{st} & C + \sqrt{D} \end{pmatrix}, \quad \mathbf{P}_2 = \frac{-1}{2\sqrt{D}} \begin{pmatrix} -C - \sqrt{D} & 2\gamma_{con} \\ 2\alpha\gamma_{st} & C - \sqrt{D} \end{pmatrix}$$

Where,

$$C = \gamma_{st} - \gamma_{con}, \quad D = C^2 + 4\gamma_{st}\gamma_{con}\alpha \quad (19)$$

From Eqs. (17) and (18), the inductive heating powers in the strands and conduit,  $Q_{st}$  [W] and  $Q_{con}$  [W], are calculated in the following way.

$$Q_{st} = \gamma_{con}^2 PNR_{st} \left\{ \omega^2 \left( \frac{-1}{\omega^2 + \lambda_1^2} + \frac{1}{\omega^2 + \lambda_2^2} \right)^2 + \left( \frac{\lambda_1}{\omega^2 + \lambda_1^2} + \frac{\lambda_2}{\omega^2 + \lambda_2^2} \right)^2 \right\}, \quad (20)$$

$$Q_{con} = \frac{PR_{con}}{4} \left\{ \omega^2 \left( \frac{C + \sqrt{D}}{\omega^2 + \lambda_1^2} - \frac{C - \sqrt{D}}{\omega^2 + \lambda_2^2} \right)^2 + \left[ \frac{\lambda_1(C + \sqrt{D})}{\omega^2 + \lambda_1^2} + \frac{\lambda_2(C - \sqrt{D})}{\omega^2 + \lambda_2^2} \right]^2 \right\}.$$

Where,

$$P = \frac{\omega^2 B_p^2 L^2}{\mu_0 D} \quad (21)$$

When there are no strands in the conduit, the governing equation for the eddy currents in the conduit becomes as follows,

$$\frac{dI_{con}}{dt} + \frac{R_{con}L}{\mu_0 S_{con}} I_{con} + \frac{j\omega B_p L}{\mu_0} e^{j\omega t} = 0. \quad (22)$$

The solution of this equation is,

$$I_{con} = \frac{\omega B_p L}{(\gamma_{con}L)^2 + (\mu_0\omega)^2} (\mu_0\omega + j\gamma_{con}L) \quad (23)$$

The heat power in the conduit,  $Q_{con}^h$  [W], is therefore calculated as follows.

$$Q_{con}^h = \frac{R_{con}(\omega B_p L)^2}{(\gamma_{con}L)^2 + (\mu_0\omega)^2} \quad (24)$$

$Q_{con}$  [W] and  $Q_{con}^h$  [W] are evaluated as  $612 B_p^2$  W and  $626 B_p^2$  W, respectively.

The decrease in the heat energy due to the coupling of the eddy currents in the strands and conduit is about 3%. The ratio of the heating powers in the strands and conduit is

evaluated to be 1.94. However, the experiment showed it is to be 1.70. They are in relative good agreement. This verifies the above calculation. The inductive heating energy can therefore be estimated by subtracting the heat energy in the conduit from the one of the conductor as follows.

$$E_h = 1.291 \times 10^{-3} \int_0^h I_h^2 dt \quad (25)$$

## 5.2 Correction of heat energy

The geometries of the inductive heaters in the stability experiment and this experiment differ to some extent<sup>9,10</sup>. The magnetic field applied to the conductor is therefore different for the same inductive heater current between these experiments.

Since the calculation carried out in 5.1 indicates the magnetic field produced by the eddy currents is much small in comparison with the applied magnetic field, we can neglect the effect from the magnetic field made by the induced eddy currents in the strands and conduit. Consequently, the magnitude of the eddy currents is almost proportional to square of the applied magnetic field at this point. The correction of the heat energy due to the difference in the geometry of the inductive heaters is carried out by assuming the heat energy per unit volume is proportional to the square of the magnetic field. The current to the inductive heater in the stability experiments,  $i_h$  [A], therefore satisfies the following equation,

$$\int_0^h i_h^2 dt = \frac{\int_0^l b_p^2 dx}{\int_0^l B_p^2 dx} \int_0^h I_h^2 dt \quad (26)$$

Where  $b_p$  [T] and  $l$  [m] show the magnetic field from the inductive heater and the length of the conductor used in the stability experiment, respectively. The relation between the heating factor and heat energy by the inductive heater used in the stability experiment is evaluated as follows from Eqs. (7), (8) and (26).

i) For the conductor,

$$E_h = 8.045 \times 10^{-3} \int_0^h i_h^2 dt. \quad (27)$$

ii) For the conduit,

$$E_h = 3.008 \times 10^{-3} \int_0^h i_h^2 dt. \quad (28)$$

iii) For the strands,

$$E_h = 5.037 \times 10^{-3} \int_0^h i_h^2 dt. \quad (29)$$

## 6. Conclusion

The inductive heating energy of the sub-size improved DPC-U conductor consisting of 27 chrome plated NbTi strands was evaluated at a magnetic field of 7 T using the calorimetric method. The heat energies put in the strands and conduit were individually estimated. The results are :

- 1) The inductive heating energy is in proportion to integration of the square of the heater current over the heating period. The proportional constants for the conductor and conduit were  $2.062 \times 10^{-3} \text{ [J/A}^2\text{s]}$  and  $0.771 \times 10^{-3} \text{ [J/A}^2\text{s]}$ , respectively.
- 2) Although the coupling between the eddy currents in the strands and conduit might have an influence on the inductive heating energy generated in the strands, this effect is negligibly small for this conductor. The proportional constant for the heat energy put in the strands is then estimated as  $1.291 \times 10^{-3} \text{ [J/A}^2\text{s]}$  from the difference of the heat energies in the conductor and conduit.

## Acknowledgments

The authors would like to thank Drs. S. Shimamoto, M. Ohta and T. Nagashima for their encouragement and support during this work. Thank should also be given to all staff members of the Superconducting Magnet Laboratory in JAERI. Showa Electric Wire & Cable Co. Ltd is gratefully acknowledged for their manufacturing contributions.

## References

1. Tsuji, H., Tada, E., Okuno, K., Ando, T., *et al.* *Proc. MT-11* Elsevier Science Publishers, Essex, UK (1990) p.806.

ii) For the conduit,

$$E_h = 3.008 \times 10^{-3} \int_0^h i_h^2 dt. \quad (28)$$

iii) For the strands,

$$E_h = 5.037 \times 10^{-3} \int_0^h i_h^2 dt. \quad (29)$$

## 6. Conclusion

The inductive heating energy of the sub-size improved DPC-U conductor consisting of 27 chrome plated NbTi strands was evaluated at a magnetic field of 7 T using the calorimetric method. The heat energies put in the strands and conduit were individually estimated. The results are :

- 1) The inductive heating energy is in proportion to integration of the square of the heater current over the heating period. The proportional constants for the conductor and conduit were  $2.062 \times 10^{-3} \text{ [J/A}^2\text{s]}$  and  $0.771 \times 10^{-3} \text{ [J/A}^2\text{s]}$ , respectively.
- 2) Although the coupling between the eddy currents in the strands and conduit might have an influence on the inductive heating energy generated in the strands, this effect is negligibly small for this conductor. The proportional constant for the heat energy put in the strands is then estimated as  $1.291 \times 10^{-3} \text{ [J/A}^2\text{s]}$  from the difference of the heat energies in the conductor and conduit.

## Acknowledgments

The authors would like to thank Drs. S. Shimamoto, M. Ohta and T. Nagashima for their encouragement and support during this work. Thank should also be given to all staff members of the Superconducting Magnet Laboratory in JAERI. Showa Electric Wire & Cable Co. Ltd is gratefully acknowledged for their manufacturing contributions.

## References

1. Tsuji, H., Tada, E., Okuno, K., Ando, T., *et al.* *Proc. MT-11* Elsevier Science Publishers, Essex, UK (1990) p.806.

ii) For the conduit,

$$E_h = 3.008 \times 10^{-3} \int_0^h i_h^2 dt. \quad (28)$$

iii) For the strands,

$$E_h = 5.037 \times 10^{-3} \int_0^h i_h^2 dt. \quad (29)$$

## 6. Conclusion

The inductive heating energy of the sub-size improved DPC-U conductor consisting of 27 chrome plated NbTi strands was evaluated at a magnetic field of 7 T using the calorimetric method. The heat energies put in the strands and conduit were individually estimated. The results are :

- 1) The inductive heating energy is in proportion to integration of the square of the heater current over the heating period. The proportional constants for the conductor and conduit were  $2.062 \times 10^{-3} \text{ [J/A}^2\text{s]}$  and  $0.771 \times 10^{-3} \text{ [J/A}^2\text{s]}$ , respectively.
- 2) Although the coupling between the eddy currents in the strands and conduit might have an influence on the inductive heating energy generated in the strands, this effect is negligibly small for this conductor. The proportional constant for the heat energy put in the strands is then estimated as  $1.291 \times 10^{-3} \text{ [J/A}^2\text{s]}$  from the difference of the heat energies in the conductor and conduit.

## Acknowledgments

The authors would like to thank Drs. S. Shimamoto, M. Ohta and T. Nagashima for their encouragement and support during this work. Thank should also be given to all staff members of the Superconducting Magnet Laboratory in JAERI. Showa Electric Wire & Cable Co. Ltd is gratefully acknowledged for their manufacturing contributions.

## References

1. Tsuji, H., Tada, E., Okuno, K., Ando, T., *et al.* *Proc. MT-11* Elsevier Science Publishers, Essex, UK (1990) p.806.

ii) For the conduit,

$$E_h = 3.008 \times 10^{-3} \int_0^h i_h^2 dt. \quad (28)$$

iii) For the strands,

$$E_h = 5.037 \times 10^{-3} \int_0^h i_h^2 dt. \quad (29)$$

## 6. Conclusion

The inductive heating energy of the sub-size improved DPC-U conductor consisting of 27 chrome plated NbTi strands was evaluated at a magnetic field of 7 T using the calorimetric method. The heat energies put in the strands and conduit were individually estimated. The results are :

- 1) The inductive heating energy is in proportion to integration of the square of the heater current over the heating period. The proportional constants for the conductor and conduit were  $2.062 \times 10^{-3}$  [J/A<sup>2</sup>s] and  $0.771 \times 10^{-3}$  [J/A<sup>2</sup>s], respectively.
- 2) Although the coupling between the eddy currents in the strands and conduit might have an influence on the inductive heating energy generated in the strands, this effect is negligibly small for this conductor. The proportional constant for the heat energy put in the strands is then estimated as  $1.291 \times 10^{-3}$  [J/A<sup>2</sup>s] from the difference of the heat energies in the conductor and conduit.

## Acknowledgments

The authors would like to thank Drs. S. Shimamoto, M. Ohta and T. Nagashima for their encouragement and support during this work. Thank should also be given to all staff members of the Superconducting Magnet Laboratory in JAERI. Showa Electric Wire & Cable Co. Ltd is gratefully acknowledged for their manufacturing contributions.

## References

1. Tsuji, H., Tada, E., Okuno, K., Ando, T., *et al.* *Proc. MT-11* Elsevier Science Publishers, Essex, UK (1990) p.806.

2. Koizumi, N., Okuno, K., Takahashi, Y., Tsuji, H., *et al.* *Cryogenics* (1994) 34 p.155.
3. Koizumi, N., Okuno, K., Takahashi, Y., Tsuji, H., *et al.* *Cryogenics* (1994) 34 p.1015.
4. Koizumi, N., Okuno, K., Takahashi, Y., Tsuji, H., *et al.* *Cryogenics* (1996) 36 p.409.
5. Steeves, M., Takayasu, M., Painter, T., Hoenig, M., *et al.* *Adv. Cryog. Eng.* (1991) 37 p.345.
6. Nishi, M., Ando, T., Tsuji, H., Hamajima, T., *et al.* *Cryogenic Engineering* (1992) 27 (3) p.36 *Cryogenics* (1993) 33 p.573.
7. Ando, T., Nakajima, H., Sasaki, T., Hiyama, Y., *et al.* *Advances in Cryogenic Engineering* (1994) Vol. 39 p.335.
8. Takahashi, Y., Koizumi, N., Wadayama, Y., Okuno, K., *et al.* *IEEE Appl. Supercond.* (1993) 3 (1) p.610.
9. Koizumi, N., Takahashi, Y. and Tsuji, H. *Cryogenics To be published.*
10. Koizumi, N., Takahashi, Y., Okuno, K., Nishi, M., *et al.* *Cryogenics* under contribution.
11. Kuroda, K. *Cryogenics* (1986) 26 p.566.
12. Davies, J. and Simpson, P. *Induction Heating Handbook* McGraw-Hill (UK) (1979).
13. Ono, M., Hamajima, K., Yamaguchi, M., Fujioka, T., *et al.* *Cryogenic Engineering* (1996) *To be published.*
14. Hirsh, M. and Smale, S. *Differential Equations, Dynamical Systems and Linear Algebra* Academic Press, New York (1974).
15. Zadeh, L. and Desoer, A. *Linear System Theory* McGraw-Hill, New York, US (1963).